# Minimum-exponents ansatz for molecular dynamics and quantum dissipation

Jin-Jin Ding, Hou-Dao Zhang, Yao Wang, Rui-Xue Xu, Xiao Zheng, and YiJing Yan

Citation: J. Chem. Phys. **145**, 204110 (2016); doi: 10.1063/1.4967964
View online: http://dx.doi.org/10.1063/1.4967964
View Table of Contents: http://aip.scitation.org/toc/jcp/145/20
Published by the American Institute of Physics

# Minimum-exponents ansatz for molecular dynamics and quantum dissipation

Jin-Jin Ding,[1,a)] Hou-Dao Zhang,[2,a)] Yao Wang,[2] Rui-Xue Xu,[2] Xiao Zheng,[2] and YiJing Yan[2,b)]

[1]*School of Chemistry and Chemical Engineering, Nantong University, Nantong, Jiangsu 226019, China*
[2]*Hefei National Laboratory for Physical Sciences at the Microscale and Department of Chemical Physics and iChEM and Synergetic Innovation Center of Quantum Information and Quantum Physics, University of Science and Technology of China, Hefei, Anhui 230026, China*

(Received 28 September 2016; accepted 5 November 2016; published online 28 November 2016)

A unified theory for minimum exponential-term ansatzes on bath correlation functions is proposed for numerically efficient and physically insightful treatments of non-Markovian environment influence on quantum systems. For a general Brownian oscillator bath of frequency $\Omega$ and friction $\zeta$, the minimum ansatz results in the correlation function a bi-exponential form, with the effective $\bar{\Omega}$ and friction $\bar{\zeta}$ being temperature dependent and satisfying $\bar{\Omega}/\Omega = (\bar{\zeta}/\zeta)^{1/2} = \bar{r}_{\rm BO}/r_{\rm BO} \le 1$, where $\bar{r}_{\rm BO} = \bar{\zeta}/(2\bar{\Omega})$ and $r_{\rm BO} = \zeta/(2\Omega)$. The maximum value of $\bar{r}_{\rm BO} = r_{\rm BO}$ can effectively be reached when $k_BT \ge 0.8\Omega$. The bi-exponential correlation function can further reduce to single-exponential form, in both the diffusion ($r_{\rm BO} \gg 1$) limit and the pre-diffusion region that could occur when $r_{\rm BO} \ge 2$. These are remarkable results that could be tested experimentally. Moreover, the impact of the present work on the efficient and accuracy controllable evaluation of non-Markovian quantum dissipation dynamics is also demonstrated. *Published by AIP Publishing.* [http://dx.doi.org/10.1063/1.4967964]

## I. INTRODUCTION

We propose a so-called minimum-dissipaton ansatz (MDA) that is closely related to the common practice on using one or few exponential function(s) to analyse dynamical properties observed in experiments and simulations in research. The involving exponents are often related to chemical reaction rates, energy relaxations, and decoherences processes. Moreover, the number of the exponential terms, and also the values of the exponents and coefficients, varies as temperature and other experimental parameters. Detailed analysis on them will not only result in rate information but also the underlying mechanisms.

The proposed MDA method in this work would also greatly facilitate the numerical implementation of the hierarchical-equations-of-motion (HEOM),[1–6] an exact and nonperturbative quantum dissipation theory. As it is operationally friendly, HEOM has been applied to various systems, including the transient quantum transport through impurities,[7–9] and coherent excitation energy transfer and nonlinear optical spectroscopy in biological pigment–protein complexes.[10–16]

Recently, Yan and co-workers developed the dissipaton-equation-of-motion (DEOM) theory.[17,18] As a quasi-particle theory for interacting environments, DEOM treats also the hybrid bath dynamics that are often experimentally measurable. These include the Fano interferences[19–21] and Herzberg–Teller vibronic couplings[22,23] in optical spectroscopies, reaction rate fluctuations in single-molecule experiments,[24,25] and transport current shot noise spectrum.[26,27] Moreover, an exact DEOM theory for *nonlinear* environment couplings has also been established.[28]

Without loss of generality, we will illustrate the to-be-developed MDA theory with a Gaussian environment, where DEOM recovers HEOM. The explicit expression for HEOM/DEOM depends on the bath correlation function in an exponential decomposition form [setting $\beta = 1/(k_BT)$ and $\hbar = 1$ hereafter],

$$\langle \hat{F}_{\rm B}(t)\hat{F}_{\rm B}(0)\rangle_{\rm B} = \frac{1}{\pi}\int_{-\infty}^{\infty} {\rm d}\omega \frac{e^{-i\omega t}J(\omega)}{1-e^{-\beta\omega}} = \sum_{k=1}^{K\to\infty}\eta_k e^{-\gamma_k t}. \quad (1)$$

The first identity is the fluctuation–dissipation theorem. The second identity is formally exact as $K \to \infty$. Conventionally, it is carried out via certain sum-over-poles decomposition methods on the individual components of the Fourier integrand, followed by the Cauchy's contour integration in the lower-half plane.[29–36] Thus, $K = N_J + N_{\rm Bose}$, with $N_J$ and $N_{\rm Bose}$ being the numbers of poles from the bath spectrum density $J(\omega)$ and the Bose function, respectively. For the case of $N_a$ dissipation modes, the total number of dynamical variables in the HEOM/DEOM formalism will be $\frac{(N_aK+L)!}{(N_aK)!L!}$. Here, $L$ denotes the truncation tier level. There has been much effort on developing efficient HEOM methods, such as the on-the-fly numerical filtering algorithm,[37] the sparse matrixes algorithm,[38] the Padé spectrum decomposition of Bose function,[35,36] the derivative-resum tier level truncation,[39] and so on. To advance DEOM/HEOM as a standard tool in computational nonlinear spectroscopy, we have also put forward a mixed Heisenberg-Schrödinger scheme.[13,18] Furthermore, the DEOM/HEOM propagator is suited perfectly for the usage of graphics processing units.[15,16] Nevertheless, efficient methods developed by now focus mainly on Drude dissipations, where

a)J.-J. Ding and H.-D. Zhang contributed equally to this work.
b)Electronic address: yanyj@ustc.edu.cn

the influence of bath assumes to be purely diffusive.[40] Existing machineries for the non-Drude environment[41–45] remain in general rather expensive.

Note that in the DEOM theory, each exponential term in Eq. (1) associates with a statistical quasi-particle, the dissipaton.[17,18] On the other hand, the $K$-space sum-over-poles expansion of the Fourier integrand is rather mathematical. This would have little relation to the common practice of using one or few exponential function(s) to physically analyse the dynamical environment influence. The MDA theory to be developed in this work aims at $K = N_J \leq 2$ and $N_{\rm B} = 0$, effectively, with the renormalized single or pair exponential terms to be more physically relevant.

In this work, the MDA refers to the bi-exponential approximation for the general of Brownian oscillator (BO) bath; see Sec. II. It could further reduce to a single-exponential form, in two well-defined and accuracy controllable limiting situations; see Sec. III. We will see that in a broad range of parameter space the proposed MDAs work very well, in comparing with the exact dynamics. We conclude this paper with Sec. IV.

## II. MINIMUM-DISSIPATON ANSATZ

The spectral density of a BO bath is given by[29,30,45]

$$J(\omega) = \frac{2\lambda\Omega^2\zeta\omega}{(\Omega^2-\omega^2)^2+(\zeta\omega)^2}. \tag{2}$$

Here, $\lambda$ is the solvation energy; $\Omega$ and $\zeta$ are the bath frequency and friction constant, respectively. Each BO mode has two poles in the lower-half plane, having

$$\gamma_1 = \frac{1}{2}(\zeta + \sqrt{\zeta^2-4\Omega^2}), \quad \gamma_2 = \frac{1}{2}(\zeta - \sqrt{\zeta^2-4\Omega^2}). \tag{3}$$

As characterized by $r_{\rm BO} \equiv \zeta/(2\Omega)$, the BO can be underdamped ($r_{\rm BO} < 1$), critically damped ($r_{\rm BO} = 1$), overdamped ($r_{\rm BO} > 1$), or strongly overdamped ($r_{\rm BO} \gg 1$), respectively.

The MDA for BO bath (MDA-BO) adopts [cf. Eq. (1)]

$$\langle \hat{F}_{\rm B}(t)\hat{F}_{\rm B}(0)\rangle_{\rm B} \approx \eta_+ e^{-\gamma_+ t} + \eta_- e^{-\gamma_- t}. \tag{4}$$

All involving parameters are complex and temperature dependent, and to be determined soon; cf. Eq. (6). The exponents take the pair form of Eq. (3),

$$\gamma_\pm = \frac{1}{2}\Big[\bar{\zeta} \pm \big(\bar{\zeta}^2 - 4\bar{\Omega}^2\big)^{\frac{1}{2}}\Big], \qquad \bar{\zeta}, \bar{\Omega} > 0. \tag{5}$$

The effective frequency and friction parameters, $\bar{\Omega}$ and $\bar{\zeta}$, will also be temperature-dependent. In this work, we propose the following three complex equations to evaluate the MDA-BO parameters:

$$\eta_+ + \eta_- = \langle \hat{F}_{\rm B}^2\rangle_{\rm B}, \tag{6a}$$

$$\frac{\eta_+}{\gamma_+} + \frac{\eta_-}{\gamma_-} = \hat{C}(0) = \lambda\Big(\frac{2\zeta}{\beta\Omega^2} - i\Big), \tag{6b}$$

$$\frac{\eta_+}{\gamma_+^2} + \frac{\eta_-}{\gamma_-^2} = -i\hat{C}'(0). \tag{6c}$$

Here, $\hat{C}(0) = \hat{C}(\omega=0)$ and $\hat{C}'(0) = {\rm d}\hat{C}(\omega=0)/{\rm d}\omega$, with

$$\hat{C}(\omega) \equiv \int_0^\infty {\rm d}t\, e^{i\omega t}\langle \hat{F}_{\rm B}(t)\hat{F}_{\rm B}(0)\rangle_{\rm B} \equiv C(\omega) + iD(\omega). \tag{7}$$

The dispersion function, $D(\omega)$ in Eq. (7), is related to the spectrum, $C(\omega) = J(\omega)/(1-e^{-\beta\omega})$, via the Kramers-Kronig relation,

$$D(\omega) = \frac{1}{\pi}\mathcal{P}\int_{-\infty}^{\infty} {\rm d}\omega' \frac{C(\omega')}{\omega-\omega'}. \tag{8}$$

Here, $\mathcal{P}$ denotes the principle part. The above relations lead to

$$\hat{C}(\omega=0) = \frac{J(\omega)}{1-e^{-\beta\omega}}\Big|_{\omega=0} - \frac{i}{2\pi}\int_{-\infty}^{\infty}{\rm d}\omega\frac{J(\omega)}{\omega}. \tag{9}$$

This gives to the last identity of Eq. (6b), given $J(\omega)$ of Eq. (2).

As described in Eqs. (6a)–(6c), the minimum-dissipaton ansatz, Eq. (4), is exact at $t = 0$, and the resultant approximates $\hat{C}(\omega)$ and $\hat{C}'(\omega)$ are also exact at $\omega = 0$.In Appendix, we present the derivations on the solutions to Eq. (4) and also the MDA-BO bath spectrum. Denote $\theta \equiv k_B T/\Omega$ and $\bar{r}_{\rm BO} = \bar{\zeta}/(2\bar{\Omega})$ hereafter. The final results are summarized as follows. First of all, the MDA-BO, Eq. (6), has the remarkable properties of [cf. Eqs. (A6) and (A13)]

$$\frac{\bar{\zeta}}{\zeta} = \frac{\bar{\Omega}^2}{\Omega^2} = \frac{\bar{r}_{\rm BO}^2}{r_{\rm BO}^2} = \frac{1+\Phi}{1+\Psi} \equiv \frac{1}{Z}. \tag{10}$$

Here,

$$\Phi \equiv \sum_{m=1}^{\infty}\frac{2}{1+4\pi m\theta(\pi m\theta + r_{\rm BO})}, \tag{11a}$$

$$\Psi \equiv 2\sum_{m=1}^{\infty}\frac{1+(2\pi m\theta)^2 - 4r_{\rm BO}^2 + \frac{r_{\rm BO}}{\pi m\theta}}{[1+(2\pi m\theta)^2]^2 - (4\pi m\theta r_{\rm BO})^2}. \tag{11b}$$

The solutions to Eq. (6) read

$$\gamma_\pm = \frac{\Omega}{Z}(r_{\rm BO} \pm \sqrt{r_{\rm BO}^2 - Z}), \tag{12a}$$

$$\eta_\pm = \lambda\Omega\Big[\theta(1+\Phi) \pm \frac{2\theta r_{\rm BO}(\Phi-1)+i}{2\sqrt{r_{\rm BO}^2-Z}}\Big]. \tag{12b}$$

Finally but not the least, the MDA-BO, Eq. (6), acquires the bath spectrum [cf. Eqs. (A15)–(A19)],

$$C(\omega) \approx \Big(\frac{1}{2} + \frac{1}{\beta\omega} + \beta\theta^2\Phi Z\omega\Big)\bar{J}(\omega), \tag{13}$$

with [cf. Eqs. (2), (A17b), and (A19)]

$$\bar{J}(\omega) = \frac{2\lambda\bar{\Omega}^2\bar{\zeta}\omega}{(\bar{\Omega}^2-\omega^2)^2+(\bar{\zeta}\omega)^2} = \frac{2\lambda\Omega^2\zeta\omega}{(\Omega^2-Z\omega^2)^2+(\zeta\omega)^2}. \tag{14}$$

The Bose function in the MDA-BO reads then

$$\frac{1}{1-e^{-\beta\omega}} \approx \Big(\frac{1}{2} + \frac{1}{\beta\omega} + \beta\theta^2\Phi Z\omega\Big)\frac{\bar{J}(\omega)}{J(\omega)}. \tag{15}$$

Unlike Matsubara and Padé expansions,[35,36] this is not universal, but specialized for Brownian oscillators.

Figure 1 shows the MDA-BO bath spectrum, C($\omega$) of Eq. (13), versus the exact ones (thin-curves), at 77 K and 300 K, illustrated for the underdamped ($r_{\rm BO} = 0.1$), critically damped ($r_{\rm BO} = 1$), and overdamped ($r_{\rm BO} = 5$) cases. The bath frequency is $\Omega = 200$ cm$^{-1}$. Apparently, the MDA-BO [Eq. (6)] offers

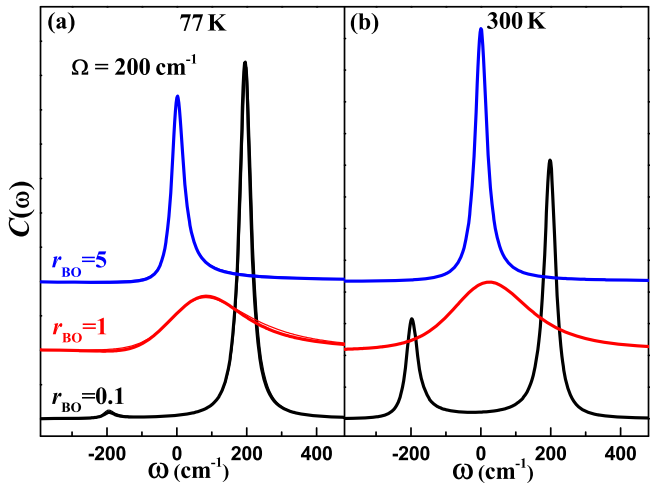


FIG. 1. The BO ansatz bath spectrums [Eq. (13)] versus the exact ones (thin-curves), at 77 K and 300 K, illustrated for the underdamped ($r_{\rm BO}$ = 0.1), critically damped ($r_{\rm BO}$ = 1), and overdamped ($r_{\rm BO}$ = 5) cases. The bath frequency is $\Omega$ = 200 cm$^{-1}$.

a truly excellent bi-exponential approximant to the BO bath correlation function.

Figure 2 depicts $Z(r_{\rm BO},\theta)$, defined in Eq. (10), and $\bar{r}_{\rm BO}(r_{\rm BO},\theta)\equiv\bar{\zeta}/(2\bar{\Omega})=r_{\rm BO}/\sqrt{Z}$, in the upper- and lower-panels, respectively, where $\theta = k_BT/\Omega$. It is noticed that in general, $Z(r_{\rm BO},\theta) > 1$. This is equivalent to $\bar{r}_{\rm BO}/r_{\rm BO} = \bar{\Omega}/\Omega = \sqrt{\bar{\zeta}/\zeta} < 1$ [cf. Eq. (10)]. Moreover, $Z \to 1$, or equivalently, $\bar{r}_{\rm BO} \to r_{\rm BO}$ around $\theta > 0.8$. This is the dashed line ($\bar{r}_{\rm BO} = r_{\rm BO}$) in the lower-right panel of Fig. 2. As inferred from Eq. (10), the classical (or a quasi-classical) bath description could be valid in the $Z \to 1$ regime.

Unlike the formally exact Eq. (1) via certain sum-over-poles expansion methods,[29–36] the MDA-BO construction on Eq. (4) via Eq. (6) represents a semiclassical bath description, which can be readily validated by the comparison between the analytical ansatz bath spectrum, Eq. (13), and the exact $C(\omega) = J(\omega)/(1-e^{-\beta\omega})$; see Fig. 1. In fact, it is found that the

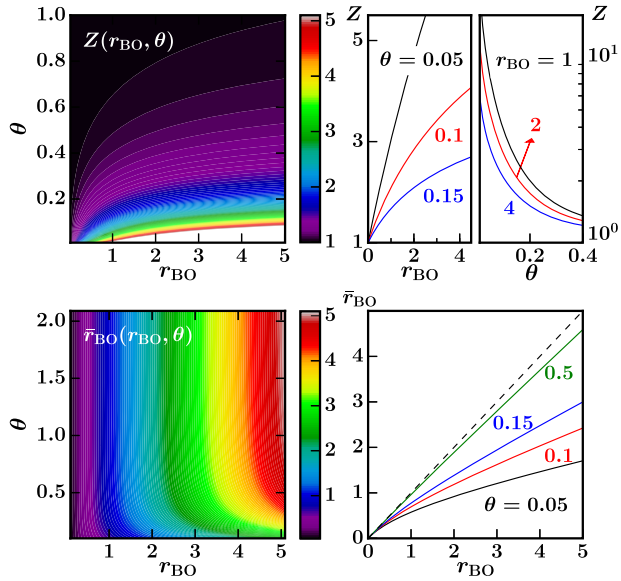


FIG. 2. The BO ansatz function, $Z(r_{\rm BO},\theta)$ (upper-panels), and the resulting $\bar{r}_{\rm BO}(r_{\rm BO},\theta)\equiv\bar{\zeta}/(2\bar{\Omega}) = r_{\rm BO}/\sqrt{Z}$ (lower-panels); see Eq. (10), with Eq. (11) where $\theta = k_BT/\Omega$. The dashed-line in the lower-right panel indicates where $\bar{r}_{\rm BO} = r_{\rm BO}$.

present MDA-BO description is valid for about $k_BT/\Omega > 0.08$, covering almost the whole range of parameter $r_{\rm BO}$. This remarkable feature will greatly facilitate the implementation of various quantum dissipation methods, such as the quantum master equations[30,46–51] and the numerical path-integral propagators.[52–54]

In this work, we demonstrate the MDA-BO [Eq. (4)] with its resulting HEOM formalism,[1–4]

$$\begin{aligned}\dot{\rho}_{n_1n_2} = &-(i\mathcal{L}_{\rm S} + n_1\gamma_+ + n_2\gamma_-)\rho_{n_1n_2}\\ &-i[\hat{Q}_{\rm S},\rho_{n_1+1,n_2}+\rho_{n_1,n_2+1}]\\ &-in_1(\eta_+\hat{Q}_{\rm S}\rho_{n_1-1,n_2}-\bar{\eta}_+^*\rho_{n_1-1,n_2}\hat{Q}_{\rm S})\\ &-in_2(\eta_-\hat{Q}_{\rm S}\rho_{n_1,n_2-1}-\bar{\eta}_-^*\rho_{n_1,n_2-1}\hat{Q}_{\rm S}).\end{aligned}\tag{16}$$

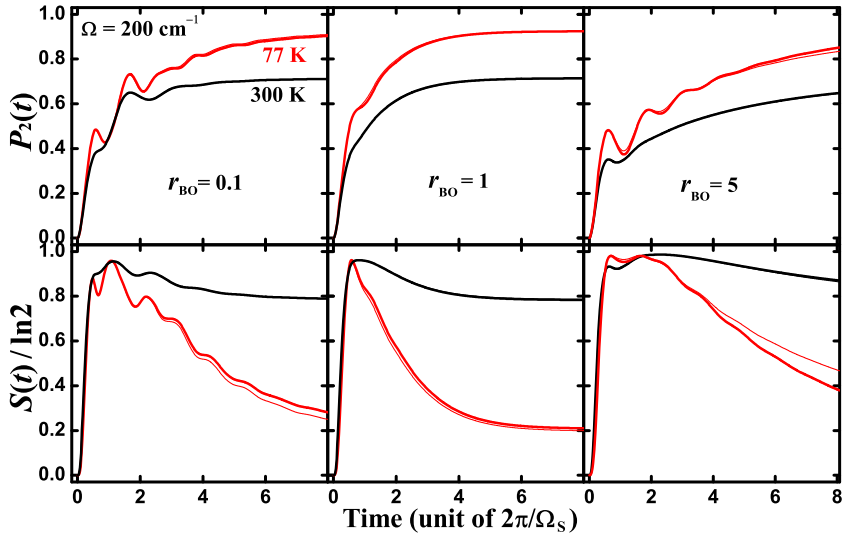


FIG. 3. Performance of the BO ansatz [Eq. (6) or (12)], for the resulting HEOM dynamics [Eq. (16)], on a spin-boson system, $H_{\rm S} = \epsilon\hat{\sigma}_z + V\hat{\sigma}_x$, with $\epsilon = V = \lambda$ = 100 cm$^{-1}$. Upper panels: $P_2(t) = \langle 2|\rho_{\rm S}|2\rangle$; lower panels: $S(t) = -{\rm tr}_{\rm S}[\rho_{\rm S}(t)\ln\rho_{\rm S}(t)]$, scaled by $S_{\rm max} = \ln 2$, the maximum entropy of a two-level system. The time is in the unit of bare system oscillation period. The exact dynamics are shown in thin-curves.

Here, $\hat{Q}_S$ denotes the system dissipation mode, through which the generalized Langevin force $\hat{F}_B$ acts on the system; $\bar{\eta}_\pm = \eta_\pm$ if $\gamma_\pm$ is real, or $\bar{\eta}_\pm = \eta_\mp$ if $\gamma_+ = \gamma_-^*$, respectively. In Eq. (16), $\{\rho_{n_1 n_2}(t)\}$, the auxiliary density operators in the original HEOM theory,[1–6] are actually the dissipaton density operators, according to their physical picture.[17,18] The DEOM theory supports also direct evaluation of hybrid bath dynamics, based on the underlying dissipaton algebra.

Figure 3 reports the resulting HEOM (16) evaluations on a spin-boson model system. Illustrated are the population transfer and entropy evolutions, at 77 K (red) and 300 K (black), for the underdamped ($r_{BO} = 0.1$), critically damped ($r_{BO} = 1$), and overdamped ($r_{BO} = 5$) cases, respectively. The bath coupling strength and frequency are fixed at $2\lambda = \Omega = 200$ cm$^{-1}$. The system Hamiltonian and dissipation mode are $H_S = \epsilon\hat{\sigma}_z + V\hat{\sigma}_x$ and $\hat{Q}_S = \sigma_z$, respectively, with $\epsilon = V = 100$ cm$^{-1}$, and $\Omega_S = 2\sqrt{\epsilon^2 + V^2}$ the transition frequency. As anticipated from Fig. 1, the evaluated dynamics, especially those at $T = 300$ K, agree excellently with the exact results that are shown in thin-curves in individual panels. Note that for $r_{BO} = 1$ and $\Omega = 200$ cm$^{-1}$, the effective $\bar{r}_{BO} = 0.8856$ and 0.9938, at $T = 77$ and 300 K, respectively.

## III. SINGLE-DISSIPATON LIMITS

### A. Strongly overdamped (Drude) bath

The Drude bath spectral density is

$$J_D(\omega) = \frac{2\lambda\gamma_D\omega}{\omega^2 + \gamma_D^2}. \tag{17}$$

The MDA-Drude would go with

$$\langle\hat{F}_B(t)\hat{F}_B(0)\rangle_B \approx \eta\, e^{-\gamma t} + 2\Delta\delta(t). \tag{18}$$

The addition of a white-noise term is in line with the common practice on an efficient evaluation of the bath influence at the moderately low temperature regime.[40,55,56]

For the Drude dissipation, $\langle\hat{F}_B^2\rangle_B$ diverges; thus Eq. (6a) will not be used. Eqs. (6b) and (6c) will only be exploited, which read now

$$\begin{aligned} \tfrac{\eta}{\gamma} + \Delta &= \hat{C}(0) = \lambda\left(\tfrac{2}{\beta\gamma_D} - i\right), \\ \tfrac{\eta}{\gamma^2} &= -i\hat{C}'(0) = D'(0) - i\tfrac{\lambda}{\gamma_D}. \end{aligned} \tag{19}$$

The identity of $C'(0) = \lambda/\gamma_D$ is used here. Again, we use the Matsubara expansion to evaluate $D'(0)$, and express the result in terms of [cf. Eq. (A11b)]

$$D'(0) = 2\beta\lambda\theta_D^2\,[1 - \Psi_D(\theta_D)]\,, \tag{20}$$

where $\theta_D = 1/(\beta\gamma_D)$ and

$$\Psi_D(\theta_D) \equiv \sum_{m=1}^{\infty} \frac{1}{\pi m\theta_D(2\pi m\theta_D + 1)}. \tag{21}$$

The solutions to Eq. (19) read then

$$\begin{aligned} &\gamma = \gamma_D, \quad \Delta = 2\lambda\theta_D\Psi_D, \\ &\eta = 2\lambda k_B T(1 - \Psi_D) - i\lambda\gamma_D. \end{aligned} \tag{22}$$

The exact value on $\mathrm{Im}\,\langle\hat{F}_B(t)\hat{F}_B(0)\rangle_B = -\lambda\gamma_D e^{-\gamma_D t}$ is recovered without approximation.

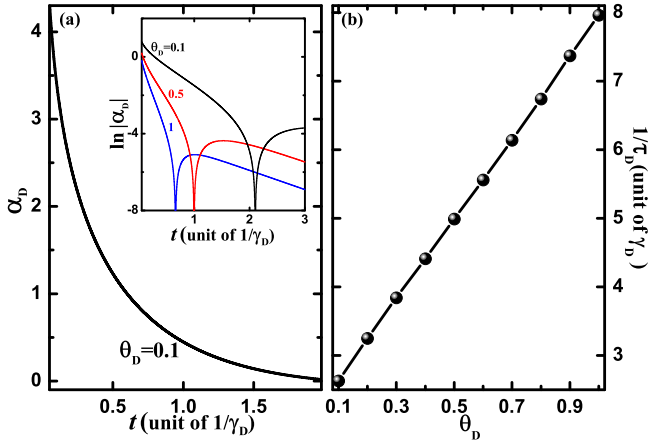


FIG. 4. (a) $\alpha_D(t;\theta_D)$ [Eq. (23)], and also $\ln|\alpha_D(t;\theta_D)|$ in the inset, at the specified values of $\theta_D = k_BT/\gamma_D$; (b) $1/\tau_D$ (in unit of $\gamma_D$), the inverse time scale of $\alpha_D(t;\theta_D)$; see text for the details.

The accuracy control function for the MDA-Drude, Eq. (18), would be

$$\alpha_D(t;\theta_D) \equiv \frac{\langle\hat{F}_B(t)\hat{F}_B(0)\rangle_B - \eta\, e^{-\gamma_D t}}{\lambda\gamma_D}. \tag{23}$$

This is a real function, as just mentioned that its imaginary part is zero. Figure 4(a) depicts $\alpha_D(t;\theta_D)$, at a representing temperature, $\theta_D = k_BT/\gamma_D = 0.1$. Note that for a Drude bath, $\langle\hat{F}_B(t\to 0)\hat{F}_B(0)\rangle_B \to \infty$; thus $\alpha_D(t;\theta_D)$ diverges at $t = 0$. Plotted in Fig. 4(a) is of $t \geq 0.05/\gamma_D$. The characteristic time scale $\tau_D$ of $\alpha_D(t;\theta_D)$ can be identified via the slope of $\ln|\alpha(t;\theta_D)|$, within the region of $t < t_D$, such that $|\alpha_D(t > t_D;\theta_D)|$ becomes negligibly small; see inset in Fig. 4(a). With the aforementioned linear analysis, we obtain $(\tau_D\gamma_D)^{-1}$ as a function of $\theta_D$, as shown in Fig. 4(b), which fits nicely by

$$(\gamma_D\tau_D)^{-1} \simeq 2.053 + 5.883\theta_D. \tag{24}$$

It is anticipated that the MDA-Drude is valid when both $\gamma_D\tau_D$ and $\tau_D/\tau_S$ are small enough, where $\tau_S$ denotes the characteristic time scale of the system in study.

For the MDA-Drude [Eq. (18)], the HEOM reads

$$\begin{aligned} \dot{\rho}_n = &-(i\mathcal{L}_S + n\gamma)\rho_n - \Delta[\hat{Q}_S,[\hat{Q}_S,\rho_n]] \\ &- i[\hat{Q}_S,\rho_{n+1}] - in(\eta\hat{Q}_S\rho_{n-1} - \eta^*\rho_{n-1}\hat{Q}_S). \end{aligned} \tag{25}$$

Figure 5 reports its performance on the same two-level system as Fig. 3, compared with the exact dynamics (thin-curves). The value $\Omega_S = 2\sqrt{2}\times 100$ cm$^{-1}$ is fixed. Illustrated are the resulting dynamics, with $\gamma_D = \Omega_S$, at three specified values of $\theta_D = k_BT/\gamma_D$. In the present study, the MDA-Drude dynamics are numerically accurate when $\theta_D > 0.5$.

### B. Highly overdamped (pre-diffusion) bath

Consider now the pre-diffusion or highly overdamped (HO) case, where $r_{BO} > 1$, or more precisely $\bar{r}_{BO} > 1$ is finite. The HO regime is then about where the faster-decay component of Eq. (4), with $\gamma_+ = (\Omega/Z)(r_{BO} + \sqrt{r_{BO}^2 - Z}) > 0$ [cf. Eq. (12a)] could be effectively replaced by a white noise that

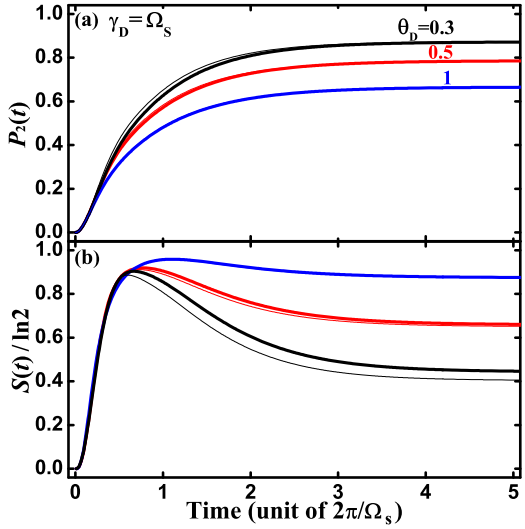


FIG. 5. Performance of the MDA–Drude [Eq. (18) with Eq. (22)], for the resulting HEOM [Eq. (25)] dynamics on (a) $P_2(t) = \langle 2|\rho_S|2\rangle$; (b) $S(t) = -\mathrm{tr}_S[\rho_S(t)\ln\rho_S(t)]$. The time unit is the bare system oscillation period. The demonstrated two–level system, $H_S$, and reorganization energy, $\lambda$, are the same as Fig. 3. The Drude damping parameter $\gamma_D = \Omega_S$, at the three specified values of $\theta_D = k_BT/\gamma_D$. The exact results are shown in thin–curves.

should be of the Caldeira–Leggett's type,[57]

$$\eta_+ e^{-\gamma_+ t} \approx 2\frac{\eta_+^{(r)}}{\gamma_+}\delta(t) - 2i\frac{\eta_+^{(i)}}{\gamma_+^2}\dot\delta(t). \tag{26}$$

The MDA-HO bath correlation function assumes then

$$\langle \hat F_B(t)\hat F_B(0)\rangle_B \approx \eta\, e^{-\gamma t} + 2\frac{\eta_+^{(r)}}{\gamma_+}\delta(t) - 2i\frac{\eta_+^{(i)}}{\gamma_+^2}\dot\delta(t)\,. \tag{27}$$

The parameters $\gamma_+ > 0$ and $\eta_+ \equiv \eta_+^{(r)} + i\eta_+^{(i)}$ had been given by the MDA-BO in Sec. II. However, the real $\gamma > 0$ and the complex parameter $\eta$ should be determined [cf. Eq. (31)]. They would deviate from $\gamma_-$ and $\eta_-$, respectively, for a certain compensation over the given white-noise approximant of Eq. (27). On the other hand, this approximant rules out the possibilities of Eq. (6a) completely, and further the imaginary part of Eq. (6b), since $\int_0^\infty \dot\delta(t)\mathrm{d}t = -\delta(0)$. Neither $\delta(0)$ nor $\dot\delta(0)$ by own is physically defined. The survivals would only be the real part of Eq. (6b) and the complex Eq. (6c) from which the MDA-HO parameters, the complex $\eta$ and the real $\gamma$, can be determined. To evaluate those survivals from Eq. (6), we exploit the identities, $2\int_0^\infty \delta(t)\mathrm{d}t = 1$, and

$$\begin{aligned}\left[2\int_0^\infty \mathrm{d}t\, e^{i\omega t}\delta(t)\right]'_{\omega=0} &= 0,\\ \left[2\int_0^\infty \mathrm{d}t\, e^{i\omega t}\dot\delta(t)\right]'_{\omega=0} &= -i.\end{aligned} \tag{28}$$

Consequently, the survival expressions from Eq. (6) for the MDA-HO, Eq. (27), read (denoting $\eta \equiv \eta_r + i\eta_i$)

$$\frac{\eta_r}{\gamma} = C(0) - \frac{\eta_+^{(r)}}{\gamma_+}, \tag{29a}$$

$$\frac{\eta}{\gamma^2} = -i\left[\hat C'(0) + \frac{\eta_+^{(i)}}{\gamma_+^2}\right]. \tag{29b}$$

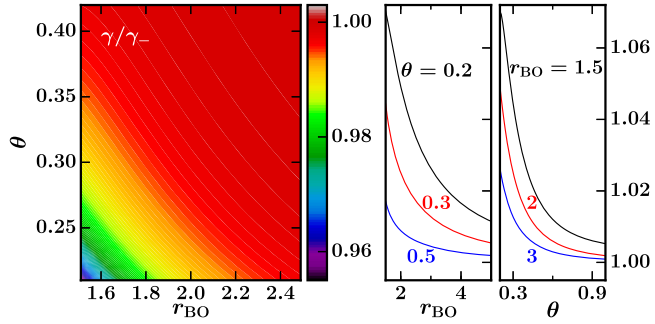


FIG. 6. The MDA-HO damping ratio, $\gamma/\gamma_-$ [Eq. (31)], as function of $r_{BO}$ and $\theta = k_BT/\Omega$. Here, $\gamma_- = (\Omega/Z)(r_{BO} - \sqrt{r_{BO}^2 - Z})$ [cf. Eq. (12a)] is also a function of $r_{BO}$ and $\theta$.

We obtain

$$\gamma = \frac{C(0) - \eta_+^{(r)}/\gamma_+}{D'(0)}, \quad \eta = -i\gamma^2\left[\hat C'(0) + \frac{\eta_+^{(i)}}{\gamma_+^2}\right]. \tag{30}$$

The values of $C(0)$, and the real and imaginary parts of $\hat C'(0) = C'(0) + iD'(0)$ were given in Eqs. (A4), (A5), and (A11b), respectively. Together with the real parts of Eqs. (6b) and (6c), which determine $\gamma_-$, we have

$$\frac{\gamma}{\gamma_-} = 1 - \frac{\eta_+^{(r)}}{\gamma_+^2 D'(0)}. \tag{31}$$

Note that $\gamma_- = (\Omega/Z)(r_{BO} - \sqrt{r_{BO}^2 - Z})$ [cf. Eq. (12a)] itself is a function of $r_{BO}$ and $\theta = k_BT/\Omega$. The above MDA-HO damping ratio, as depicted in Fig. 6, shows a relatively mild dependence on $r_{BO}$ and $\theta$. Evidently, $\gamma \to \gamma_-$, when either $r_{BO} \gg 1$ or $\theta \gg 1$.

For the MDA-HO [Eq. (27)], the HEOM reads

$$\begin{aligned}\dot\rho_n = &-(i\mathcal{L}_S + n\gamma + \delta\mathcal{R})\rho_n - i[\hat Q_S, \rho_{n+1}]\\ &- in(\eta\hat Q_S\rho_{n-1} - \eta^*\rho_{n-1}\hat Q_S),\end{aligned} \tag{32}$$

with

$$\mathcal{R}\hat O = \frac{\eta_+^{(r)}}{\gamma_+}[\hat Q_S,[\hat Q_S,\hat O]] + \frac{\eta_+^{(i)}}{\gamma_+^2}[\hat Q_S,\{[H_S,\hat Q_S],\hat O\}]. \tag{33}$$

Figure 7 demonstrates the performance of the resulting HEOM dynamics. The same test system of Figs. 3 and 5 is illustrated, with the two specified overdamped values of $r_{BO} = \zeta/(2\Omega)$, at $\theta = k_BT/\Omega = 0.1$. Apparently, the MDA-HO results shown here reproduce those of the MDA-BO [Eq. (6)], which are practically exact. The higher $\theta$ or $r_{BO}$ the better, which is in line with the fact that $\theta_{HO} \equiv \zeta/(\beta\Omega^2) = 2r_{BO}\theta = 2r_{BO}\theta_2(r_{BO} - \sqrt{r_{BO}^2 - 1})$, where $\theta_2 = 1/(\beta\gamma_2)$, with $\gamma_2$ being given in Eq. (3).

To conclude this subsection, let us comment on the accuracy control function for the MDA-HO [Eq. (27)],

$$\alpha_{HO}(t) \equiv \frac{\langle \hat F_B(t)\hat F_B(0)\rangle_B - \eta\, e^{-\gamma t}}{\lambda\Omega}. \tag{34}$$

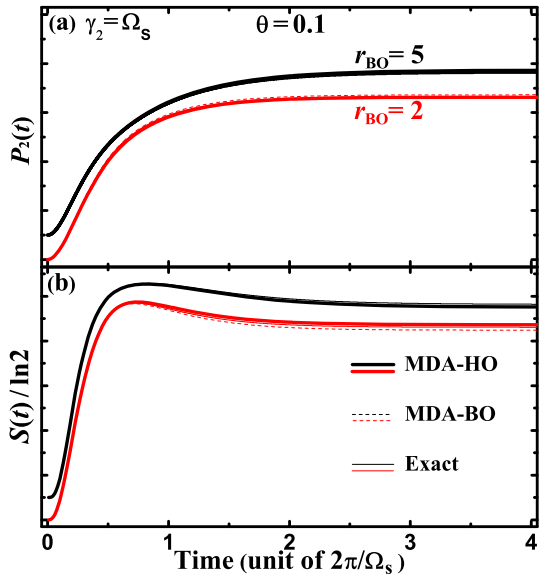


FIG. 7. Performance of the MDA-HO [Eq. (27) with Eq. (30)], for the resulting HEOM [Eq. (32)] dynamics on (a) $P_2(t) = \langle 2|\rho_S|2\rangle$; (b) $S(t) = -\mathrm{tr}_S[\rho_S(t)\ln\rho_S(t)]$. The time unit is the bare system oscillation period. The demonstrated two-level system, $H_S$, and reorganization energy, $\lambda$, are the same as Figs. 3 and 5. Other BO bath parameters are of $\gamma_2 = \frac{1}{2}(\zeta - \sqrt{\zeta^2 - 4\Omega^2}) = \Omega_S$ [cf. Eq. (3)], with the two specified overdamped values of $r_{BO} = \zeta/(2\Omega)$, at $\theta = k_BT/\Omega = 0.1$. The curves with the higher $r_{BO}$ are lift up by 0.1. The MDA-BO and the exact results are shown in dotted-curves and thin-curves, respectively.

This is a complex function, $\alpha_{HO}(t) = \alpha^{(r)}_{HO}(t) + i\alpha^{(i)}_{HO}(t)$. The MDA-HO [Eq. (27)] adopts the approximations,

$$\alpha^{(r)}_{HO}(t) \approx \frac{2\eta^{(r)}_+}{\lambda\Omega\gamma_+}\delta(t), \tag{35a}$$

$$\alpha^{(i)}_{HO}(t) \approx -\frac{2\eta^{(i)}_+}{\lambda\Omega\gamma^2_+}\dot\delta(t). \tag{35b}$$

With the identity of $\int_t^\infty \dot\delta(t)\mathrm{d}t = -\delta(t)$, we may recast Eq. (35b) as

$$\tilde\alpha^{(i)}_{HO}(t) \equiv \gamma_+ \int_t^\infty \mathrm{d}t\, \alpha^{(i)}_{HO}(t) \approx \frac{2\eta^{(i)}_+}{\lambda\Omega\gamma_+}\delta(t). \tag{36}$$

The characteristic time for the MDA-HO would then be $\tau_{HO} \equiv \max(\tau^{(r)}_{HO}, \tilde\tau^{(i)}_{HO})$, with $\tau^{(r)}_{HO}$ and $\tilde\tau^{(i)}_{HO}$ being those of $\alpha_{HO}(t)$ and $\tilde\alpha^{(i)}_{HO}(t)$, respectively, which can be individually analysed; see Fig. 4 and discussions there. The MDA-HO would be valid when both $\gamma\tau_{HO}$ and $\tau_D/\tau_S$ are small enough, where $\tau_S$ denotes the characteristic time scale of the system in study.

## IV. CONCLUDING REMARKS

In summary, we proposed a protocol, Eq. (6), for Brownian oscillator correlation function to be expressed in a bi-exponential form, Eq. (4). Proposed are also its two variations, Eqs. (19) and (29), for the diffusion limit and the pre-diffusion regime, respectively, where the correlation functions, Eqs. (18) and (27), are effectively of single-exponent. All these minimum ansatzes are accuracy controllable, and support a broad range of parameter space. The resulting exponents and pre-exponential coefficients are generally all temperature-dependent. In particular, for a general Brownian oscillator bath of frequency $\Omega$ and friction $\zeta$, the resulting effective $\bar\Omega$ and friction $\bar\zeta$ satisfy $\bar\Omega/\Omega = (\bar\zeta/\zeta)^{1/2} \le 1$. The maximum ratio here can effectively be reached when $k_BT \ge 0.8\Omega$. In this regime, $\bar\Omega = \Omega$ and $\bar\zeta = \zeta$, and the classical (or a quasi-classical) bath description could be valid. The present MDA-BO of Eq. (4) via Eq. (6) represents a semiclassical bath description, which is valid for about $k_BT > 0.08\Omega$, covering almost the whole range of parameter $r_{BO} = \zeta/(2\Omega)$; see Figs. 1 and 2 and the comments there. The reported features in these two figures for Eq. (10) could be tested experimentally.

The impact of the present work on the efficient evaluation of non-Markovian quantum dissipation dynamics is demonstrated with the accurate HEOM evaluations on quantum dissipative dynamics. Apparently, the minimum-dissipaton ansatz and its two variations are all semiclassical bath theories. They will also facilitate the implementation of other quantum dissipation methods, such as the numerical path integral influence functional propagators[52–54] and quantum master equations.[30,46–51] For the Brownian oscillator baths, all these ansatzes have analytical expressions. However, the detailed construction of minimum-dissipaton ansatz could be varied for different bath models. For example, Eq. (6c) would not be applicable for the class of Ohmic baths,[29,58] since its spectral density, $J(\omega) \propto \omega|\omega|^{s-1}e^{-|\omega|/\omega_c}$, has the first-order discontinuity at $\omega = 0$. An alternative condition will be needed. On the other hand, one may numerically decompose a general $J(\omega)$ in the multiple-Brownian-oscillators form.[30,31,45] The composite bath correlation function in the ansatz-based exponential expansion is then followed by using the analytical results of this work. Nevertheless, the principle of minimum-dissipaton ansatz is general, and it is related closely to the common practice of using one or few exponential function(s) to analyse dynamical properties observed in experiments and simulations.

## ACKNOWLEDGMENTS

The support from the Natural Science Foundation of China (Nos. 21373191, 21633006, and 21303090), the Ministry of Science and Technology (Nos. 2016YFA0400900 and 2016YFA0200600), and the Fundamental Research Funds for the Central Universities (Nos. 2030020028 and 2340000074) is gratefully acknowledged.

## APPENDIX: DERIVATIONS OF EQS. (10)–(14)

From Eqs. (6a) and (6b), we have

$$\eta_\pm = \pm\frac{\gamma_\pm\langle\hat F^2_B\rangle_B - \bar\Omega^2\hat C(0)}{\sqrt{\bar\zeta^2 - 4\bar\Omega^2}}. \tag{A1}$$

Substitute it to Eq. (6c), followed by some simple algebra, we obtain

$$\bar\zeta\hat C(0) + i\bar\Omega^2\hat C'(0) = \langle\hat F^2_B\rangle_B. \tag{A2}$$

The solution to this complex equation is

$$\bar{\zeta} = \frac{C'(0)\langle \hat{F}_{\rm B}^2\rangle_{\rm B}}{C(0)C'(0)+D(0)D'(0)}, \tag{A3a}$$

$$\bar{\Omega}^2 = \frac{-D(0)\langle \hat{F}_{\rm B}^2\rangle_{\rm B}}{C(0)C'(0)+D(0)D'(0)}. \tag{A3b}$$

The identity $\hat{C}(\omega) = C(\omega) + iD(\omega)$ is used here.

The exact values for $C(0)$ and $D(0)$, given in the last expression of Eq. (6), read [noting that $\theta = 1/(\beta\Omega)$]

$$C(0) = 4\lambda\theta r_{\rm BO}, \qquad D(0) = -\lambda. \tag{A4}$$

It is also easy to obtain

$$C'(0) = \left(\frac{J(\omega)}{1-e^{-\beta\omega}}\right)'_{\omega=0} = \frac{2\lambda r_{\rm BO}}{\Omega}. \tag{A5}$$

As $\bar{\zeta}/\bar{\Omega}^2 = -C'(0)/D(0)$ via Eq. (A3), we obtain immediately the following properties,

$$(\bar{\zeta}/\zeta)^{\frac{1}{2}} = \bar{\Omega}/\Omega = \bar{r}_{\rm BO}/r_{\rm BO}. \tag{A6}$$

Here, $\bar{r}_{\rm BO} \equiv \bar{\zeta}/(2\bar{\Omega})$.

The exact values of $\langle \hat{F}_{\rm B}^2\rangle_{\rm B}$ and $D'(0)$ can be evaluated via the identity,

$$\begin{aligned}\langle \hat{F}_{\rm B}(t)\hat{F}_{\rm B}(0)\rangle_{\rm B} &= \frac{1}{\pi}\int_{-\infty}^{\infty} {\rm d}\omega\, e^{-i\omega t}\frac{J(\omega)}{1-e^{-\beta\omega}} \\ &= \eta_1 e^{-\gamma_1 t} + \eta_1 e^{-\gamma_2 t} + \sum_{m=1}^{\infty}\check{\eta}_m e^{-\check{\gamma}_m t}.\end{aligned} \tag{A7}$$

While $\gamma_1$ and $\gamma_2$ [Eq. (3)] arise from the poles of $J(\omega)$ in the lower-half plane, $\{\check{\gamma}_m = 2\pi m/\beta\}$ are the Matsubara frequencies, by which the Bose function is expanded as

$$\frac{1}{1-e^{-\beta\omega}} = \frac{1}{2} + \frac{1}{\beta\omega} + \frac{2}{\beta}\sum_{m=1}^{\infty}\frac{\omega}{\omega^2+\check{\gamma}_m^2}. \tag{A8}$$

Note that[4,18]

$$\check{\eta}_m = -i(2/\beta)J(-i\check{\gamma}_m) = \check{\eta}_m^*, \tag{A9}$$

due to the antisymmetry of the spectrum function, From Eq. (A7), we have

$$\langle \hat{F}_{\rm B}^2\rangle_{\rm B} = \eta_1 + \eta_2 + \sum_{m=1}^{\infty}\check{\eta}_m, \tag{A10a}$$

$$D'(0) = {\rm Re}\left(\frac{\eta_1}{\gamma_1^2} + \frac{\eta_2}{\gamma_2^2}\right) + \sum_{m=1}^{\infty}\frac{\check{\eta}_m}{\check{\gamma}_m^2}. \tag{A10b}$$

After some elementary (but rather tedious) algebra we obtain the expressions,

$$\langle \hat{F}_{\rm B}^2\rangle_{\rm B} = 2\lambda\Omega\theta[1+\Phi(r_{\rm BO},\theta)], \tag{A11a}$$

$$D'(0) = \frac{2\lambda\theta}{\Omega}[4r_{\rm BO}^2 - 1 - \Psi(r_{\rm BO},\theta)], \tag{A11b}$$

where

$$\Phi \equiv \sum_{m=1}^{\infty}\frac{2}{1+4\pi m\theta(\pi m\theta + r_{\rm BO})}, \tag{A12a}$$

$$\Psi \equiv 2\sum_{m=1}^{\infty}\frac{1+(2\pi m\theta)^2 - 4r_{\rm BO}^2 + \frac{r_{\rm BO}}{\pi m\theta}}{[1+(2\pi m\theta)^2]^2 - (4\pi m\theta r_{\rm BO})^2}. \tag{A12b}$$

These are Eq. (11). Applying Eqs. (A4), (A5), and (A11) to Eq. (A3a), we obtain

$$\frac{\bar{\zeta}}{\zeta} = \frac{1+\Phi}{1+\Psi} \equiv \frac{1}{Z}. \tag{A13}$$

It together with Eq. (A6) is the relation in Eq. (10), which leads immediately to Eq. (12a).

Substituting Eqs. (A4) and (A11a) for Eq. (A1), together with identities, $\sqrt{\bar{\zeta}^2 - 4\bar{\Omega}^2} = 2(\Omega/Z)\sqrt{r_{\rm BO}^2 - Z}$ and $\bar{\Omega}^2 Z = \Omega^2$, we obtain

$$\begin{aligned}\eta_\pm &= \pm\frac{2\lambda\Omega\theta(1+\Phi)\gamma_\pm - \bar{\Omega}^2(4\lambda\theta r_{\rm BO} - i\lambda)}{2(\Omega/Z)\sqrt{r_{\rm BO}^2 - Z}} \\ &= \pm\lambda\Omega\left[\frac{2\theta(1+\Phi)(\gamma_\pm Z/\Omega) - 4\theta r_{\rm BO} + i}{2\sqrt{r_{\rm BO}^2 - Z}}\right].\end{aligned} \tag{A14}$$

Together with Eq. (12a) we obtain Eq. (12b).

Turn now to Eqs. (13) and (14), the property of the ansatz bath spectrum. From Eq. (4), we have

$$\begin{aligned}\hat{C}(\omega) &\approx \frac{\eta_+}{\gamma_+ - i\omega} + \frac{\eta_-}{\gamma_- - i\omega} \\ &= \frac{(\eta_+\gamma_- + \eta_-\gamma_+) - i(\eta_+ + \eta_-)\omega}{\gamma_+\gamma_- - \omega^2 - i(\gamma_+ + \gamma_-)\omega} \\ &= \frac{\bar{\Omega}^2\hat{C}(0) - i\langle \hat{F}_{\rm B}^2\rangle_{\rm B}\,\omega}{\bar{\Omega}^2 - \omega^2 - i\bar{\zeta}\omega}.\end{aligned} \tag{A15}$$

The last expression is obtained by using Eqs. (6a) and (6b). Its real part is the spectrum and reads

$$C(\omega) \approx \bar{S}(\omega) + \frac{1}{2}\bar{J}(\omega), \tag{A16}$$

where [cf. the second expression in Eq. (6b)]

$$\bar{S}(\omega) \equiv \frac{2\lambda\zeta\bar{\Omega}^4 + (\beta\bar{\zeta}\Omega^2\langle \hat{F}_{\rm B}^2\rangle_{\rm B} - 2\lambda\zeta\bar{\Omega}^2)\omega^2}{\beta\Omega^2[(\bar{\Omega}^2-\omega^2)^2 + (\bar{\zeta}\omega)^2]}, \tag{A17a}$$

$$\bar{J}(\omega) \equiv \frac{2\lambda\bar{\Omega}^2\bar{\zeta}\omega}{(\bar{\Omega}^2-\omega^2)^2 + (\bar{\zeta}\omega)^2}. \tag{A17b}$$

Together with Eqs. (10) and (A11a), we obtain

$$\frac{\bar{S}(\omega)}{\bar{J}(\omega)} = \frac{1}{\beta\omega} + \theta^2\Phi(r_{\rm BO},\theta)Z(r_{\rm BO},\theta)(\beta\omega). \tag{A18}$$

Moreover, we can recast Eq. (A17b) as

$$\bar{J}(\omega) = \frac{2\lambda\Omega^2\zeta\omega}{(\Omega^2 - Z\omega^2)^2 + \zeta^2\omega^2}. \tag{A19}$$

This is Eq. (14). Applying the above two equations to Eq. (A16), we obtain Eq. (13). We have thus completed the derivations for Eqs. (10)–(14).

[1] Y. Tanimura, Phys. Rev. A **41**, 6676 (1990).
[2] Y. Tanimura, J. Phys. Soc. Jpn. **75**, 082001 (2006).
[3] R. X. Xu, P. Cui, X. Q. Li, Y. Mo, and Y. J. Yan, J. Chem. Phys. **122**, 041103 (2005).
[4] R. X. Xu and Y. J. Yan, Phys. Rev. E **75**, 031107 (2007).
[5] Y. A. Yan, F. Yang, Y. Liu, and J. S. Shao, Chem. Phys. Lett. **395**, 216 (2004).
[6] J. S. Jin, X. Zheng, and Y. J. Yan, J. Chem. Phys. **128**, 234703 (2008).
[7] X. Zheng, J. S. Jin, and Y. J. Yan, J. Chem. Phys. **129**, 184112 (2008).
[8] X. Zheng, J. S. Jin, and Y. J. Yan, New J. Phys. **10**, 093016 (2008).

[9]X. Zheng, J. S. Jin, S. Welack, M. Luo, and Y. J. Yan, J. Chem. Phys. **130**, 164708 (2009).
[10]A. Ishizaki and Y. Tanimura, J. Chem. Phys. **125**, 084501 (2006).
[11]A. Ishizaki and Y. Tanimura, J. Phys. Chem. A **111**, 9269 (2007).
[12]L. P. Chen, R. H. Zheng, Q. Shi, and Y. J. Yan, J. Chem. Phys. **132**, 024505 (2010).
[13]J. Xu, R. X. Xu, D. Abramavicius, H. D. Zhang, and Y. J. Yan, Chin. J. Chem. Phys. **24**, 497 (2011).
[14]L. P. Chen, R. H. Zheng, Y. Y. Jing, and Q. Shi, J. Chem. Phys. **134**, 194508 (2011).
[15]C. Kreisbeck, T. Kramer, M. Rodríguez, and B. Hein, J. Chem. Theory Comput. **7**, 2166 (2011).
[16]B. Hein, C. Kreisbeck, T. Kramer, and M. Rodríguez, New J. Phys. **14**, 023018 (2012).
[17]Y. J. Yan, J. Chem. Phys. **140**, 054105 (2014).
[18]Y. J. Yan, J. S. Jin, R. X. Xu, and X. Zheng, Front. Phys. **11**, 110306 (2016).
[19]U. Fano, Phys. Rev. **124**, 1866 (1961).
[20]Y. Zhang, T.-T. Tang, C. Girit, Z. Hao, M. C. Martin, A. Zettl, M. F. Crommie, Y. R. Shen, and F. Wang, Nature **459**, 820 (2009).
[21]T.-T. Tang, Y. Zhang, C.-H. Park, B. Geng, C. Girit, Z. Hao, M. C. Martin, A. Zettl, M. F. Crommie, S. G. Louie, Y. R. Shen, and F. Wang, Nat. Nanotechnol. **5**, 32 (2010).
[22]H. D. Zhang, Q. Qiao, R. X. Xu, and Y. J. Yan, "Solvent-induced polarization dynamics and coherent two-dimensional spectroscopy: Dissipation equation of motion approach," Chem. Phys. (published online 2016).
[23]H. D. Zhang, Q. Qiao, R. X. Xu, and Y. J. Yan, "Effects of Herzberg-Teller vibronic coupling on coherent excitation energy transfer," J. Chem. Phys. **145**, 204109 (2016).
[24]H. Yang, G. Luo, P. Karnchanaphanurach, T. M. Louie, I. Rech, S. Cova, L. Xun, and X. S. Xie, Science **302**, 262 (2003).
[25]W. Min, G. Luo, B. J. Cherayil, S. C. Kou, and X. S. Xie, Phys. Rev. Lett. **94**, 198302 (2005).
[26]A. A. Clerk, M. H. Devoret, S. M. Girvin, F. Marquardt, and R. J. Schoelkopf, Rev. Mod. Phys. **82**, 1155 (2010).
[27]J. S. Jin, S. K. Wang, X. Zheng, and Y. J. Yan, J. Chem. Phys. **142**, 234108 (2015).
[28]R. X. Xu, Y. Liu, H. D. Zhang, and Y. J. Yan, "Hybrid system-environment dynamics with a non-Gaussian bath coupling: Exact dissipation theory versus extended Zusman equation," arXiv:1608.07774 [physics.chem.ph].
[29]U. Weiss, *Quantum Dissipative Systems*, Series in Modern Condensed Matter Physics, 3rd ed. (World Scientific, Singapore, 2008), Vol. 13.
[30]Y. J. Yan and R. X. Xu, Annu. Rev. Phys. Chem. **56**, 187 (2005).
[31]C. Meier and D. J. Tannor, J. Chem. Phys. **111**, 3365 (1999).
[32]A. Croy and U. Saalmann, Phys. Rev. B **80**, 073102 (2009).
[33]J. Xu, R. X. Xu, M. Luo, and Y. J. Yan, Chem. Phys. **370**, 109 (2010).
[34]T. Ozaki, Phys. Rev. B **75**, 035123 (2007).
[35]J. Hu, R. X. Xu, and Y. J. Yan, J. Chem. Phys. **133**, 101106 (2010).
[36]J. Hu, M. Luo, F. Jiang, R. X. Xu, and Y. J. Yan, J. Chem. Phys. **134**, 244106 (2011).
[37]Q. Shi, L. P. Chen, G. J. Nan, R. X. Xu, and Y. J. Yan, J. Chem. Phys. **130**, 084105 (2009).
[38]D. Hou, S. K. Wang, R. L. Wang, L. Z. Ye, R. X. Xu, X. Zheng, and Y. J. Yan, J. Chem. Phys. **142**, 104112 (2015).
[39]H. D. Zhang and Y. J. Yan, J. Chem. Phys. **143**, 214112 (2015).
[40]J. J. Ding, J. Xu, J. Hu, R. X. Xu, and Y. J. Yan, J. Chem. Phys. **135**, 164107 (2011).
[41]Y. Tanimura and S. Mukamel, J. Phys. Soc. Jpn. **63**, 66 (1994).
[42]M. Tanaka and Y. Tanimura, J. Phys. Soc. Jpn. **78**, 073802 (2009).
[43]M. Tanaka and Y. Tanimura, J. Chem. Phys. **132**, 214502 (2010).
[44]K. B. Zhu, R. X. Xu, H. Y. Zhang, J. Hu, and Y. J. Yan, J. Phys. Chem. B **115**, 5678 (2011).
[45]J. J. Ding, R. X. Xu, and Y. J. Yan, J. Chem. Phys. **136**, 224103 (2012).
[46]A. G. Redfield, Adv. Magn. Opt. Reson. **1**, 1 (1965).
[47]Y. J. Yan, F. Shuang, R. X. Xu, J. X. Cheng, X. Q. Li, C. Yang, and H. Y. Zhang, J. Chem. Phys. **113**, 2068 (2000).
[48]Y. J. Yan, Annu. Rep. Prog. Chem., Sect. C: Phys. Chem. **94**, 397 (1998).
[49]W. M. Zhang, T. Meier, V. Chernyak, and S. Mukamel, J. Chem. Phys. **108**, 7763 (1998).
[50]M. Yang and G. R. Fleming, Chem. Phys. **282**, 163 (2002).
[51]Y. H. Hwang-Fu, W. Chen, and Y. C. Cheng, Chem. Phys. **447**, 46 (2015).
[52]N. Makri and D. E. Makarov, J. Chem. Phys. **102**, 4600 (1995).
[53]N. Makri and D. E. Makarov, J. Chem. Phys. **102**, 4611 (1995).
[54]N. Makri, A. Nakayama, and N. J. Wright, J. Theor. Comput. Chem. **3**, 391 (2004).
[55]A. Ishizaki and Y. Tanimura, J. Phys. Soc. Jpn. **74**, 3131 (2005).
[56]R. X. Xu, B. L. Tian, J. Xu, Q. Shi, and Y. J. Yan, J. Chem. Phys. **131**, 214111 (2009).
[57]A. O. Caldeira and A. J. Leggett, Physica A **121**, 587 (1983).
[58]A. Leggett, S. Chakravarty, A. Dorsey, M. Fisher, A. Garg, and W. Zwerger, Rev. Mod. Phys. **59**, 1 (1987).